*Scientific Journal of the Ternopil National Technical University*
*2026, vol. 121, no. 1, pp. 76–87,*
*ISSN: 2522-4433 Print, ISSN: 2522-4441 Online*
*https://doi.org/10.33108/visnyk_tntu2026.01.076*

*Submitted: 2025-12-15 | Revised: 2026-02-28 | Accepted: 2026-03-24*



# Analysis of the Stress-Strain State of Steel Solid-Web and Perforated I-Beams Used in Pitched Roof Structures

**Mykola Pidgurskyi [1*], Ivan Pidgurskyi [1], Denys Bykiv [1], Danylo Liubovitskyi [1], Yurii Rudyak [2]**

[1] Ternopil Ivan Puluj National Technical University, Ternopil, Ukraine univ@tntu.edu.ua

[2] I. Horbachevsky Ternopil National Medical University, Ternopil, Ukraine university@tdmu.edu.ua

***** Corresponding author dbikiv@gmail.com

***Abstract:*** *The paper presents a numerical investigation of the stress-strain state of steel solid-web and perforated I-beams in pitched roof systems using the finite element method (FEM) implemented in the ANSYS software environment. Single-pitch and double-pitch beams configurations were analysed under different boundary conditions (hinged and fixed supports at both ends) and roof inclinations varying from 0° to 45°, typical for industrial buildings. The principal parameters of the stress-strain state were analysed, namely deflections and equivalent (von Mises) stresses along the beam flanges, as well as equivalent stresses around the web openings. The results show that the largest deflections occur in hinged beams, while fixed significantly reduces them. For most configurations, maximum deflections are located at mid-span; however, in rigidly fixed double-pitched beams, they shift toward the quarter span. Perforated beams exhibit higher stiffness compared to solid counterparts. The distribution of equivalent stresses in perforated beams is non-uniform due to the presence of openings and local stress concentrations, which necessitated evaluation based on averaged values. Fixed beams, particularly double-pitched ones, demonstrate substantially lower average stress levels in flanges than hinged systems. Maximum stresses in perforated beams occur around end openings and generally decrease with increasing slope, with the most pronounced reduction observed in rigidly fixed double-pitched beams.*

***Keywords:*** *pitched roofs, perforated I-beams, stress-strain state, finite element method.*

## 1. INTRODUCTION

I-beams are among the most efficient structural elements in construction due to the rational cross-sectional geometry and their ability to resist significant bending moments. They are widely used as roof or floor beams in public, administrative and industrial buildings, as well as in multi-storey parking structures.

The efficiency of solid horizontal I-beams depends on the applied loading and is generally limited to spans of 3–24 m (Fig. 1(a)) [1, 2]. For shorter spans, it is more practical to employ alternative profiles (channels, hollow structural sections, etc.), whereas for longer spans roof trusses are typically adopted. Although trusses allow covering large spans, they are characterized by considerable structural depth and high fabrication labour intensity.

With the ongoing optimisation of steel structures, increasing attention is being paid to lightweight beams with corrugated, slender or perforated web [1]. Among these, perforated beams (Fig. 1(b, c)) are the most economical, as they are fabricated from hot rolled sections and require only cutting and welding operations [3–6]. Increasing the overall depth due to perforation enhances both strength and stiffness compared with the original solid profiles while simultaneously reducing structural weight. This makes perforated beams suitable for spanning distances of 30 m and more [7–10].

a) [8] b) [9] c) [10]

**Figure 1.** Elements of pitched roof systems formed by solid-web (a), single-pitched (b) and double-pitched (c) perforated steel beams.

### 1.1. Problem statement

Roofs of industrial and agricultural production facilities are generally designed with a slope. Pitched roofs have several advantages compared with flat roofs, including simplified drainage, improved natural ventilation, reduced waterproofing requirements and the possibility of installing photovoltaic modules without additional supporting systems.

At the same time, flat roofs or roofs with a slope of less than 5% require additional waterproofing measures to prevent moisture penetration into the interior space of the building or into the thermal insulation layer. Insufficient sealing leads to material moisture accumulation, deterioration of thermal insulation performance and accelerated corrosion. For this reason, manufacturers of roofing systems specify a minimum allowable slope.

Since roofs of production buildings, depending on their technological purpose, are designed with a certain inclination, there is a need to investigate the stress-strain state of steel solid-web and perforated beams under inclined positioning in order to determine effective parameters of support conditions, structural configuration, and roof slope angle.

The objective of the study is to analyse the influence of roof slope on the strength and stiffness characteristics of beams and to establish parameters ensuring their efficient structural performance. The work considers solid-web and perforated I-beams in horizontal, single-pitch and double-pitch configurations, with the inclination angles ranging from 0° to 45° under hinged and fixed support conditions.

### 1.2. Review of previous studies

In most numerical and experimental studies on perforated I-beams, hinged supports are considered under the action of locally concentrated or uniformly distributed loads acting perpendicular to the longitudinal axis of the element. In such cases, the transverse bending behaviour of the beam is analysed [6, 8, 9, 14–20]. For these beams, maximum deflections occur at midspan and may be significant, requiring an increase in section depth to satisfy stiffness requirements. To reduce deflections and stresses along the beam length, various structural solutions are employed, such as introducing roof inclination, providing thrust action or applying fixed-end restraint.

In studies [21–23] perforated beams were investigated under a complex stress-strain state arising from the formation of a pitched roof. To provide thrust in the upper part of the structure, a prestressed steel tie was used. The results demonstrated the effectiveness of such systems and allowed identification of stress distribution features in support zones and tie connection nodes.

Paper [24] examined the behaviour of various perforated members (I-beams, channels, and thin-walled Z-sections) subjected not only to transverse bending but also to biaxial bending. This enabled a more comprehensive assessment of perforated beam performance under loads applied outside the principal plane, which is typical for roof purlins of industrial buildings with large roof slopes.

In study [25–27] analytical and experimental investigations of steel columns fabricated from perforated I-sections of different lengths and under various boundary conditions were carried out. The elements were considered as centrally and eccentrically compressed members with small and large eccentricities causing bending effects. Although such solutions do not significantly reduce stresses in the column, the slenderness and stability characteristics improve depending on perforation parameters, while maintaining a lower structural weight.

When the inclination angle exceeds 45°, compressive forces begin to dominate in the element and the member effectively behaves as an inclined column. Therefore, in most beam studies the slope range is limited to 45°, within which the member retains its function primarily as a bending element.

It should also be noted that the most optimal perforated beam configurations are obtained by considering the stress-strain state in the vicinity of openings in perforated beams [20, 28–30].

## 2. METHODS

### 2.1. Theoretical aspects of research

The study considers two fundamentally different variants of beam support and beam-to-column connection, since depending on column stiffness the structural scheme may vary from a simply supported beam with sliding hinges at the ends to a fixed-end beam working with thrust action. In practice, the actual behaviour of the member is typically located between these limiting cases.

A simply supported beam with a sliding hinge does not develop thrust forces and the primary internal force is the bending moment with its maximum at midspan (Fig. 2(a)). For a fixed-end beam, extreme bending moments occur both at midspan and at the supports (Fig. 2(b)).

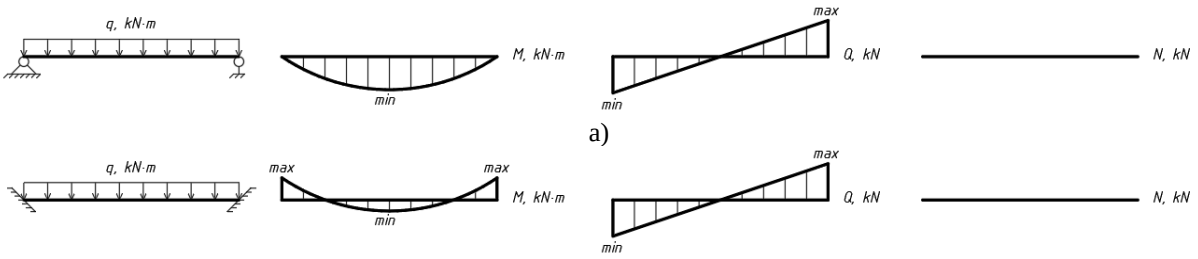


**Figure 2.** Internal forces diagrams of horizontal hinged (a) and fixed (b) beams

For pitched beams, the internal force diagrams are similar to those of horizontal beams; however, for both support schemes additional axial forces arise, which increase with the inclination angle (Fig. 3(a, b)).

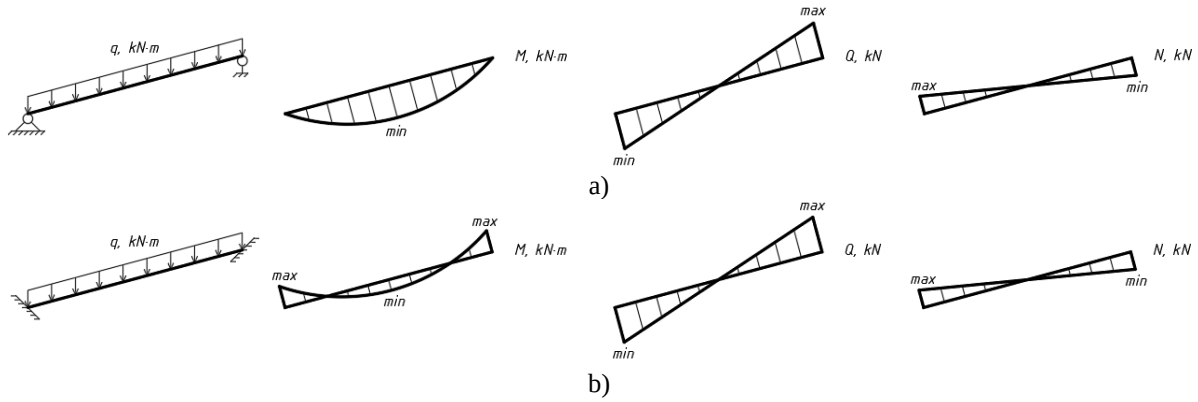


**Figure 3.** Internal forces diagrams of single-pitched hinged (a) and fixed (b) beams

For double-pitched beams with a sliding hinge at the supports and a rigid apex joint, the maximum bending effects occur near the central region of the span (Fig. 4(a)). Under fixed-end restraint, compressive forces become dominant, while the bending moment extrema occur at the supports and at midspan with one sign and in the quarter-span regions with the opposite sign (Fig. 4(b)).

Thus, depending on the type of beams and the support conditions, different internal force values occur in the cross-sections, leading to variations in the stress-strain state of the beams, especially in perforated members where openings act as stress concentrators.

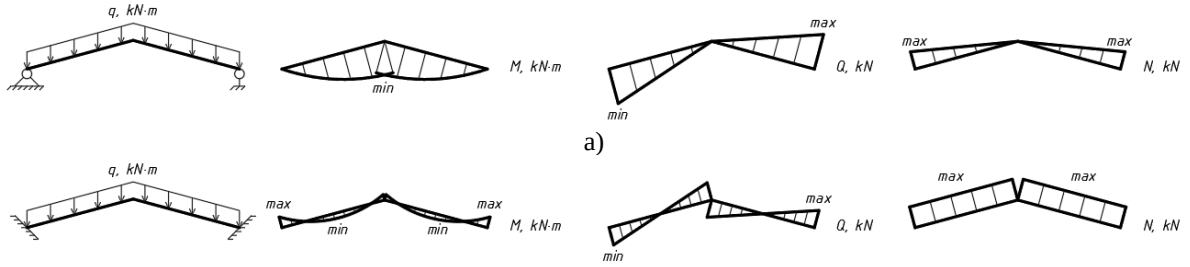


**Figure 4.** Internal forces diagrams of double-pitched hinged (a) and fixed (b) beams

## 2.2. Methodology, parameters of beams and boundary conditions

The stress-strain state of solid-web and perforated steel I-beams in inclined position was modelled using the finite element method implemented in the ANSYS software environment. Three-dimensional models were created with an average element size of 20 mm (Fig. 5(a)). The structural material was structural steel S345 [31].

The analysis included determination of vertical displacements, normal stresses, shear stresses, and equivalent stresses according to the von Mises criterion. All results were monitored along the upper and/or lower flange of the I-beam near each openings. Maximum stress values were recorded and average stresses were additionally evaluated to eliminate the influence of local stress concentration peaks. A separate analysis was also performed for stresses around the perforation openings, where maximum internal forces occur according to the force diagrams (see fig. 2–4), namely at the end opening, the midspan opening and the quarter-span opening.

Beam supports were modelled by restricting displacements at the beam ends. For hinged support, displacements along the X, Y, and Z axes were restrained at one end, while at the opposite end only the Y and Z displacements were restrained. For fixed-end restraint with thrust action, both displacements and rotations were restrained in all directions at both ends (Fig. 5(b)).

The investigated system corresponds to a roof of a production building with a span of 24 m and a beam spacing of 4 m. The total load, including the weight of the roof, bracing system and snow cover, was represented by a uniformly distributed load of 6.6 kN/m applied to the top flange of the beam (see fig. 5(b)).

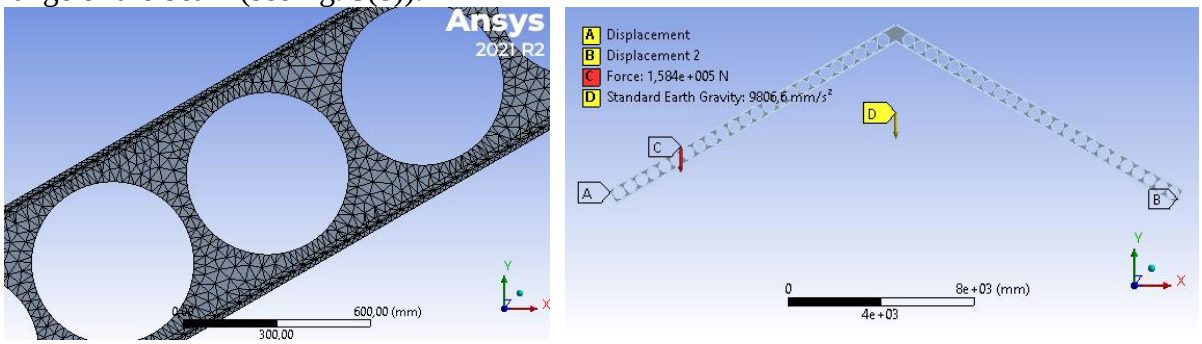


**Figure 5.** Finite element mesh (a) and boundary conditions (b) of a double-pitched perforated beam.

The self-weight of the structure was included automatically, which is essential because increasing the slope increases the actual beam length and mass, significantly affecting the resulting stress-strain state.

To reduce stress concentration, additional end stiffeners with a thickness of 20 mm were modelled at the beam ends (Fig. 6(a, b)). This dimension ensures numerical mesh stability and reliability of the results. The central joint of the beam was modelled as a butt-welded connection without additional plates.

The investigated perforated beam was fabricated by cutting and sequential welding of the original rolled IPE 400 section. The perforation opening diameter was d = 518 mm, the opening spacing s = 570 mm and the overall depth of the perforated beam h = 657.6 mm (see fig. 6(b)).

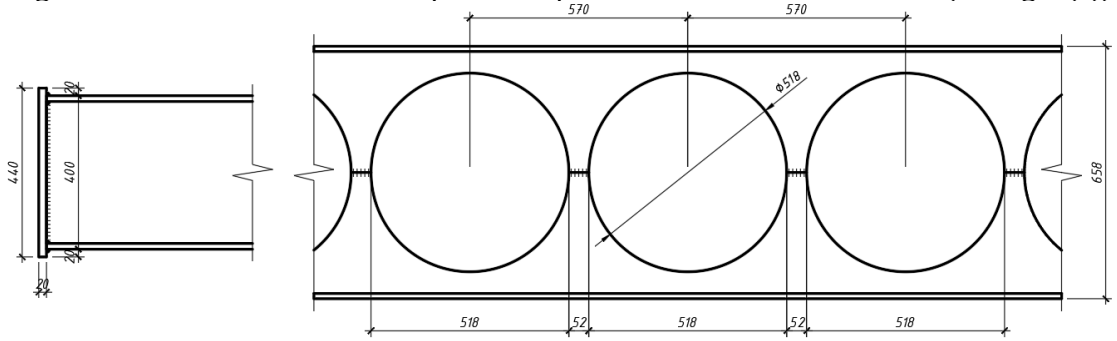


a) b)

**Figure 6.** Geometric parameters of solid-web (a) and perforated (b) I-beams.

## 3. RESULTS AND DISCISSION

A numerical investigation of the stress-strain state of single-pitched and double-pitched I-beams, both solid-web and perforated, was carried out under various boundary conditions. It was established that the beam mass increases significantly with increasing slope: for a single-pitched beam, the mass at a slope of 20° increases by 6% and at 45° by almost 30% compared with the horizontal beam.

### 3.1. Analysis of deflections

The deformation analysis showed that the largest deflections occur in single-pitched and double-pitched solid beams with hinged support (Fig. 7(a)), whereas the smallest deflections occur in double-pitched solid and perforated beams with fixed-end support (Fig. 7(b)). The variation of deflections along the beam length differs for hinged and fixed connections (Fig. 8(a, b)). For hinged supports, deflection gradually increases and reaches a maximum at midspan. For fixed single-pitched beams, deflections grow less intensively near the supports, but closer to midspan the behaviour becomes similar to hinged supported beams. For fixed double-pitched beams, deflections significantly decrease as the slope increases, and their maximum values occur not at midspan but closer to the quarter-span region.

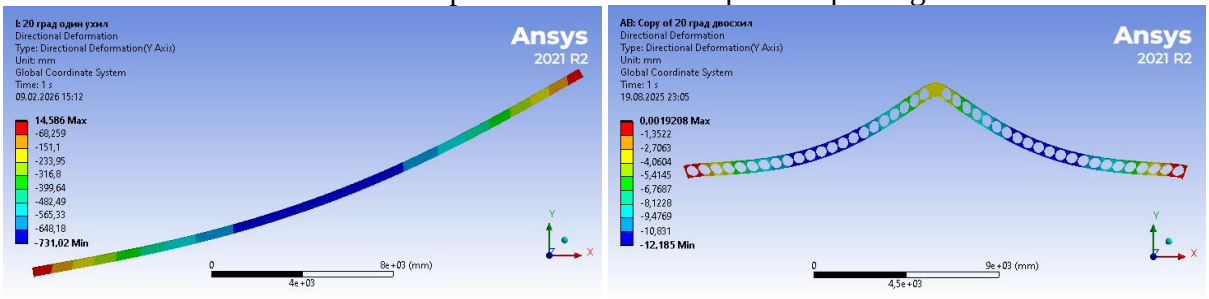


a) b)

**Figure 7.** Deformed shape (to of a solid-web single-pitched hinged beam (a) and a perforated fixed double-pitched beam (b) (slope 20°) scale).

For all hinged and fixed single-pitched beams, the following tendency is observed (Fig. 9 (a)): maximum deflections occur at a slope of 45° and minimum at 0°. For fixed perforated double-pitched beams, the tendency is opposite (Fig. 9 (b)): smaller slopes produce larger deflections. For fixed solid-web beams, deflections decrease as the slope changes from 0° to 25°, after which they slightly increase.

Figures 8 and 9 indicate that the deflections of some investigated beams exceed the normative limits (for a 24 m span the allowable deflection equals l/250, i.e., 96 mm). Therefore, certain configurations do not satisfy the Serviceability limit state (SLS). However, the obtained data are comparative in nature and allow evaluation of the influence of varying parameters on structural behaviour. The large dispersion of results is associated with differences in boundary conditions and beam types.

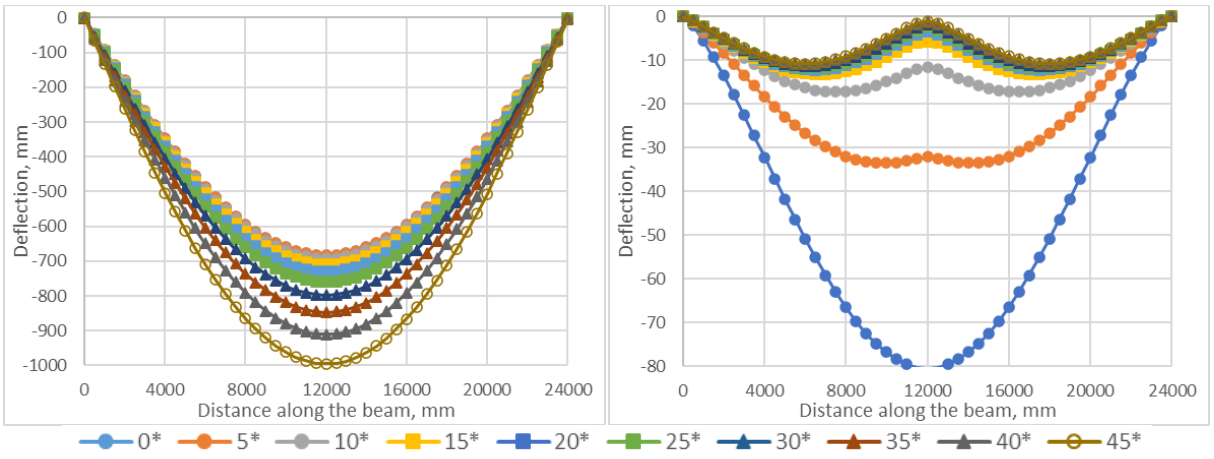


a) b)

**Figure 8.** Variation of deflection values along the beams: a solid-web single-pitched hinged beam (a) and a perforated fixed double-pitched beam (b) with changing slope

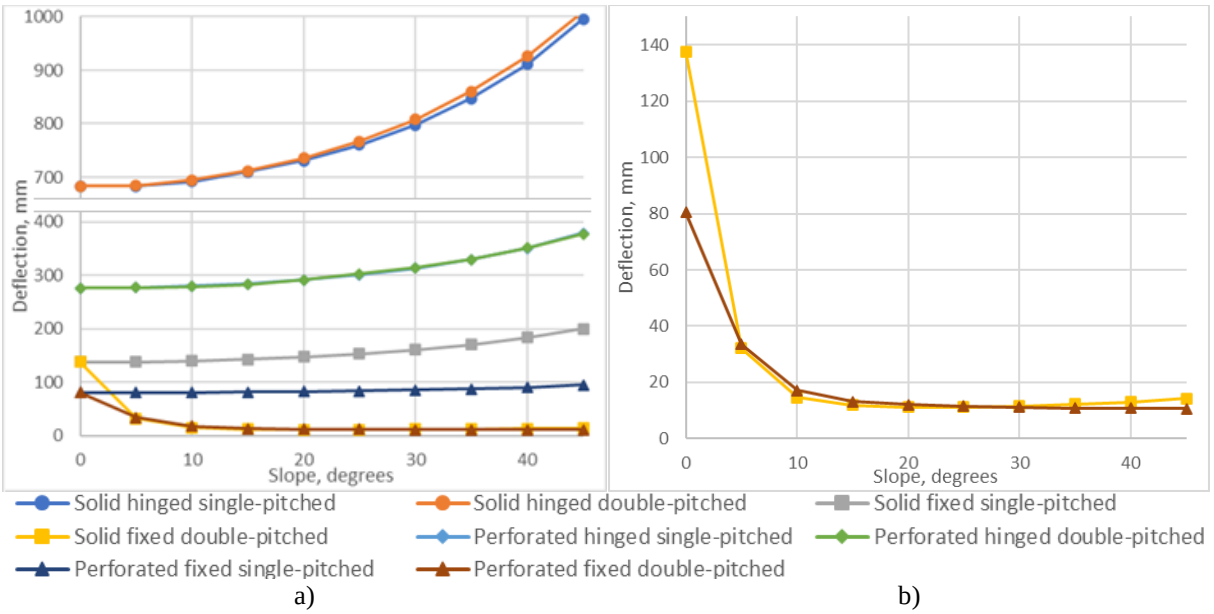


a) b)

**Figure 9.** Variation of maximum deflections of all beams with changing slope (a); only solid-web and perforated fixed double-pitched beams (b).

The stiffness analysis showed that for hinged single-pitched and double-pitched beams the deflections are approximately the same and vary mainly due to self-weight. Fixing the beam ends reduces deflections by more than 70%, depending on beam type (solid or perforated) and slope magnitude. For fixed double-pitched beams, maximum deflections occur in the quarter-span rather than at midspan as in the other beam types.

It was also found that single-pitched and double-pitched perforated beams with hinged support experience 59.6–62.7% smaller deflections than solid-web beams. single-pitched perforated beams with fixed restraint exhibit 41.6–52.6% smaller deflections than solid ones.

For fixed double-pitched beams, within slopes of 5°–25° the deflections of solid-web beams are 3.2–14.5% smaller than those of perforated beams, while for slopes of 30°–45° the opposite is observed: perforated beams show 3.4-24.6% smaller deflections. Among all analysed configurations, fixed double-pitched beams demonstrate the lowest deflections.

### 3.2. Analysis of streses

During the analysis of stresses along the lower and upper flanges, it was observed that for single-pitched perforated beams with hinged supports (Fig. 10 (a, b)) the stress distribution follows the general principles of structural mechanics, that is the stresses increase smoothly toward the mid-span. However, in perforated beams the equivalent stresses along the flanges exhibit a zigzag pattern (see fig. 10 (a)). This behaviour is explained by the variation of beam stiffness along its length due to the presence of web openings. Therefore, the evaluation was performed using averaged stresses within one amplitude interval (Fig. 10 (b, c, d)), as well as averaged stresses along the entire beam length (Fig. 11) occurring in the flanges.

The highest average stresses were obtained for single-pitched and double-pitched beams with hinged support. Under these conditions, stresses in perforated beams are 39.5–41.9% lower than in solid-web beams. The difference between single-pitch and double-pitched beams with hinged support is insignificant (up to 4% depending on slope).

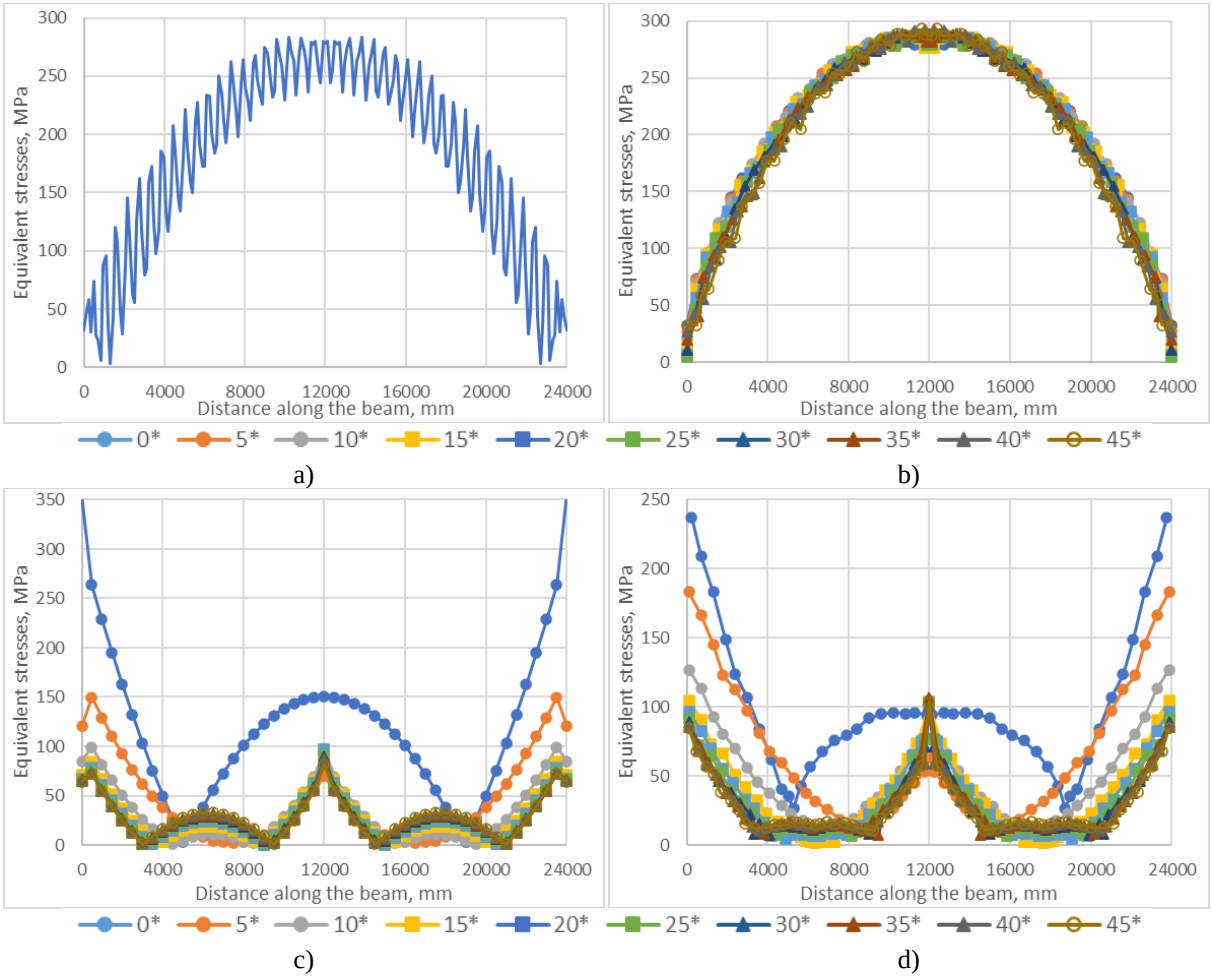


**Figure 10.** Variation of equivalent stresses along the lower flange: perforated horizontal beam (all values shown) (a) and single-pitched hinged beams (average values shown) (b); solid-web (c) and perforated (d) fixed double-pitched beams with changing slope

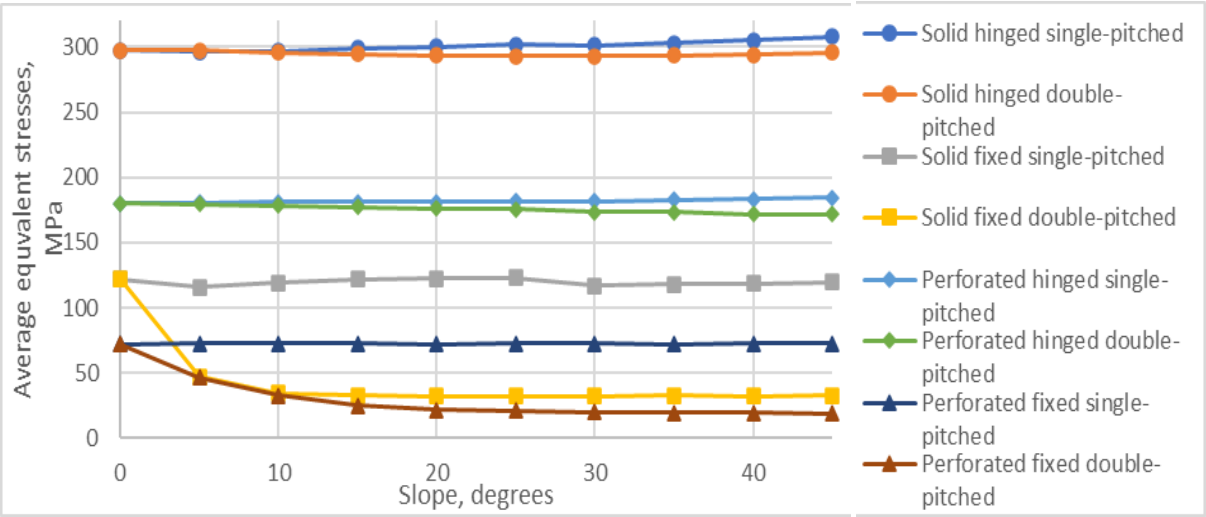


**Figure 11.** Variation of average equivalent stresses along the entire lower flanges of beams with changing slope.

Beams with fixed support experience significantly lower stresses compared with hinged beams: for single-pitched solid beams stresses decrease by 49–59% and for double-pitched beams by 84–89%. A similar tendency is observed for perforated beams, where fixed restraint reduces stresses by 61–69%.

The lowest average stresses (as well as deflections) occur in fixed double-pitched beams. Under identical loading conditions, perforated beams demonstrate 8–49% lower stresses than solid-web beams. It was also established that with hinged support the stresses in single-pitched and double-pitched beams are almost identical, whereas with fixed restraint double-pitched beams experience 70–73% lower stresses than single-pitched beams. In general, average equivalent stresses are almost independent of the slope under identical support and loading conditions, even considering the change in self-weight.

For perforated beams, maximum equivalent stresses around perforation openings were also investigated. The analysed regions correspond to locations of maximum internal forces according to the force diagrams (see fig. 2–4), namely the end opening, the midspan opening and the quarter-span opening.

For all beam types and support conditions, the maximum equivalent stresses occur around the end openings (Fig. 12 (a)). The trends of stress variation around the end opening and the quarter-span opening (Fig. 12 (b)) are similar; however, for fixed perforated double-pitched beams stresses decrease rapidly for slopes from 0° to 10° and then more gradually. For other beam types, stresses may either increase or decrease but the overall tendency from 0° to 45° is a smooth reduction.

A different behaviour is observed for the midspan's openings (Fig. 12 (c)). In hinged single-pitched and double-pitched beams, maximum equivalent stresses gradually increase with slope; at 40° they are about 13% higher than at 0°. In fixed single-pitched beams, stresses around the midspan opening vary only slightly (within 7%). In fixed double-pitched beams, stresses sharply increase between 0° and 10° (by 53%), reach a peak level that remains nearly constant up to 30° and then gradually decrease toward 45% (by about 18%).

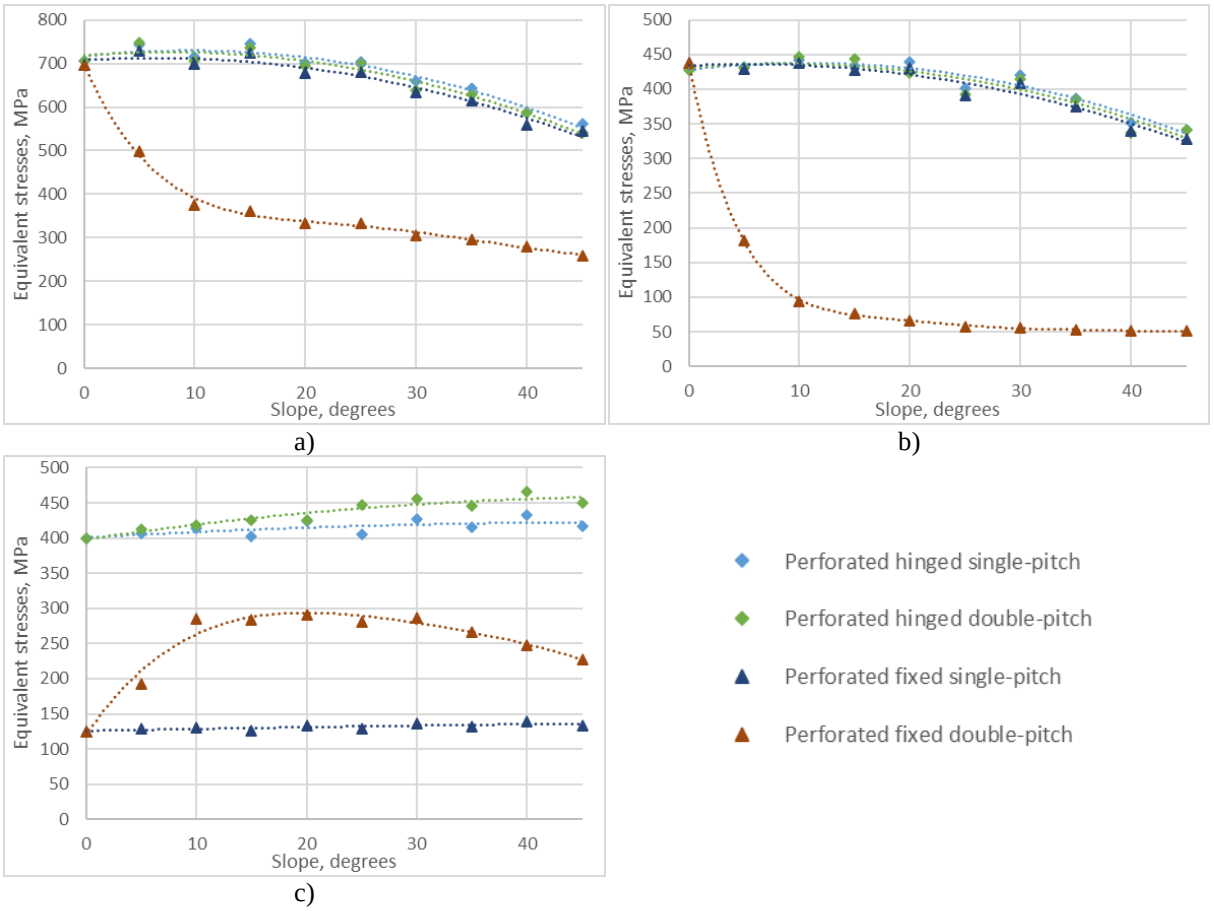


**Figure 12.** Variation of maximum equivalent stresses around the end opening (a), the quarter-span opening (b) and the midspan opening (c) with changing slope.

## 4. CONCLUSIONS

The stress-strain state of steel solid-web and perforated I-beams under varying configuration, pitch angles and boundary conditions was analysed.

It was established that the smallest deflection values are observed in rigidly fixed double-pitched beams, both solid-web and perforated. For inclination angles ranging from 5° to 25°, solid beams exhibit higher stiffness, whereas for slopes between 30° and 45°, perforated beams demonstrate greater stiffness.

For perforated beams, a significant dispersion of equivalent stresses along the flanges was observed over short distances due to stress redistribution around web openings; therefore, the results were evaluated using averaged equivalent stresses.

The highest average equivalent stresses in the I-beam flanges occur in hinged support beams, while in perforated beams they are 39.5–41.9% lower than in solid-web ones. The lowest average flange equivalent stresses occur in rigidly fixed beams, especially double-pitched structures, where stresses are 70–73% lower than in single-pitched beams.

It was determined that in perforated beams the maximum stresses occur around the openings nearest to the support. For fixed double-pitched perforated beams, increasing slope from 0° to 10° reduces stresses around the openings nearest to the support but simultaneously increases stresses near the midspan openings.

**Author Contributions:** Conceptualization: Mykola Pidgurskyi; Methodology: Denys Bykiv, Ivan Pidgurskyi; Software: [Denys Bykiv]; Validation: [Ivan Pidgurskyi]; Formal analysis: Mykola

Pidgurskyi, Yurii Rudyak; Writing – original draft preparation: Denys Bykiv, Danylo Liubovitskyi; Writing – review and editing: Ivan Pidgurskyi, Yurii Rudyak; Supervision: Mykola Pidgurskyi.

**Funding:** This research received no external funding.

**Conflicts of Interest:** The authors declare no conflicts of interest.

**Data Availability Statement:** The data that support the findings of this study are available from the corresponding author upon reasonable request.

**Declaration of Generative AI and AI-assisted technologies in the writing process:** The authors declare that no generative AI or AI-assisted technologies were used in the writing of this manuscript.

## REFERENCES

[1] G.D. Lorenzo, A. Formisano, G. Terracciano, R Landolfo Span-Depth Ratios for the preliminary structural design of steel beams: The case of European hot-rolled I sections without lateral-torsional buckling. Engineering Structures, vol. 345, 2025, 20 p. https://doi.org/10.1016/j.engstruct.2025.121504

[2] Z. Yang, Y. Chen, F. Zhou, L. Gardner, L. Guo-Qiang Testing and cross-section design of hot-rolled steel I-section beams under moment gradients, Engineering Structures, 2025, vol. 338, 120610. https://doi.org/10.1016/j.engstruct.2025.120610.

[3] A. Derlatka, P. Lacki Experimental study and numerical simulation of cellular I-beam manufactured using refill friction stir spot welding technology. Thin-Walled Structures, 2024, vol. 200. 111890. https://doi.org/10.1016/j.tws.2024.111890.

[4] S. Tas, F. Erdal, O. Tunca, R. Ozcelik Effect of geometry on flexural behavior of optimal designed web-expanded beams. Journal of Constructional Steel Research, 2024, vol. 215, 108500. https://doi.org/10.1016/j.jcsr.2024.108500.

[5] S. Sarfarazi, R. Shamass, M. Rabi, I. Abarkan, F. P. V. Ferreira, K. D. Tsavdaridis Inverse machine learning for the design of perforated beams: Parent section and material prediction. Engineering Applications of Artificial Intelligence, 2026, vol 164. 113275. https://doi.org/10.1016/j.engappai.2025.113275

[6] M. H. Haddad, A. Tanoumand, M. R. Mashayekhi, A. Majdi, A. S. Movahhed, E. N. Farsangi Develop a hybrid metaheuristic algorithm for the cost optimization of castellated beam. Engineering Computations, 2025, vol. 43, pp. 263–291. https://doi.org/10.1108/EC-05-2025-0458.

[7] ACB and Angelina beams. A new generation of beams with large web openings // ArcelorMittal Europe - Long products. ArcelorMittal, Luxembourg, 2020. 64 p.

[8] I. Pidgurskyi, V. Slobodian, D. Bykiv, M. Pidgurskyi (2021) Investigation of the stress-strain state of beams with different types of web perforation. Scientific Journal of TNTU (Tern.), vol. 103, no 3, pp. 79–87. https://doi.org/10.33108/visnyk_tntu2021.03.079

[9] Sameer S. Fares P.E., S.E., P. Eng, John Coulson, P.E., David W. Dinehart, Ph.D Castellated and cellular beam design. AISC design guide 31. American institute of steel construction, Chicago, Illinois, 2016, 110 p.

[10] EN 1993-1-13:2022 2005 Eurocode 3: Design of steel structures – Part 1–13: Rules for beams with large web openings, European committee for standardization, Brussels, 2022, 43 p.

[11] Hafif Çelik Depolar. ARK Çelik Yapilar. URL: http://arkyapi.net/urunler/hafif-celik-depolar/ (accessed: 29 March 2026).

[12] Clear Span Westok Rafters. ASD Westok. URL: https://asd.ltd/westok/clear-span-westok-rafters/ (accessed: 29 March 2026).

[13] Cellular & Castellated Beams. K. Liaromatis Structural Steelwork. URL: https://www.liaromatis.com/cellular-and-castellated-beams/ (accessed: 29 March 2026).

[14] M. Pidgurskyi, I. Pidgurskyi, M. Stashkiv, V. Ihnatieva, S. Danylchynko, D. Bykiv, O. Pidluzhnyi Peculiarities of studying the stress-strain state of structural steel perforated beams using the finite element method. Scientific Journal of TNTU (Tern.), 2023, vol. 111, no. 3, pp. 126–138. https://doi.org/10.33108/visnyk_tntu2023.03.126.

[15] K.D. Tsavdaridis, C. D'Mello Optimisation of novel elliptically-based web opening shapes of perforated steel beams. Journal of Constructional Steel Research. Elsevier Science, 2012, vol. 76, pp. 39–53. https://doi.org/10.1016/j.jcsr.2012.03.026.

[16] K.F. Chung, T.C.H. Liu, A.C.H. Ko Steel beams with large web openings of various shapes and sizes: an empirical design method using a generalized moment-shear interaction. Journal of Constructional Steel Research, vol. 59, 2003, pp. 1117–1200. https://doi.org/10.1016/S0143-974X(03)00029-4.

[17] A.A.R. Zainal, B.A. Izzuddin Meshless local buckling analysis of steel beams with irregular web openings. Engineering Structures, 2013, 50. pp. 197–206. https://doi.org/10.1016/j.engstruct.2012.10.006.

[18] A.I. Naji, M. Al-Shamaa Structural behavior of innovative castellated steel beams: experimental and numerical analysis of double and zigzag castellated patterns. Results in Engineering. 2025, vol. 27. 106259. https://doi.org/10.1016/j.rineng.2025.106259

[19] P.S. Kumar, S.S. Gowri, A.F.D. Gracy, B. Gayathiri Experimental Study on Behaviour of Steel Beams Subjected to Impact Loading. Procedia Structural Integrity, 2025, vol. 70, pp. 43–50. https://doi.org/10.1016/j.prostr.2025.07.024.

[20] T. Al-Dafafea, S. Durif, A. Bouchaïr, E. Fournely Experimental study of beams with stiffened large web openings. Journal of Constructional Steel Research, 2019, vol. 154, pp 149–160. https://doi.org/10.1016/j.jcsr.2018.11.026.

[21] V. Romaniuk, L. Bezniuk, V. Supruniuk, O. Kononchuk, O. Meshcheryakova, A. Sorochak Experimental studies of a steel rafter arch with a perforated top chord. Procedia Structural Integrity, vol. 59, 2024, pp. 479–486 https://doi.org/10.1016/j.prostr.2024.04.068.

[22] V. Romaniuk, L. Bezniuk, V. Supruniuk, O. Kononchuk, O. Meshcheryakova, A. Sorochak Features of the work of continuous perforated beams near intermediate supports. Procedia Structural Integrity, vol. 59, 2024, pp. 471–478 https://doi.org/10.1016/j.prostr.2024.04.067.

[23] A.E. Orun, M.A. Guler Effect of hole reinforcement on the buckling behaviour of thin-walled beams subjected to combined loading. Thin-Walled Structures, 2017, vol. 118, pp. 12–22. https://doi.org/10.1016/j.tws.2017.04.034.

[24] V.V. Romanyuk, V.B. Vasilenko Stress state of perforated elements operating under oblique bending conditions. Resource-efficient materials, structures, buildings and constructions: collection of scientific papers, issue 29, 2014, pp. 322–333. (In Ukrainian).

[25] H.H. El-Tobgy, A.B.B. Abu-Sena, M.W. Fares Experimental and parametric investigation of castellated steel beam-column in various expansion ratios, lengths and loading conditions, Structures, vol. 33, 2021, pp. 484–507. https://doi.org/10.1016/j.istruc.2021.04.053.

[26] J. Gu, S. Cheng Shear effect on buckling of cellular columns subjected to axially compressed load. Thin-Walled Structures, 2016, vol. 98, pp. 416–420. https://doi.org/10.1016/j.tws.2015.10.019.

[27] D. Sonck, J. Belis Weak-axis flexural buckling of cellular and castellated columns. Journal of Constructional Steel Research, 2016. vol. 124, pp. 91–100. https://doi.org/10.1016/j.jcsr.2016.05.002

[28] M.I. Pidgurskyi, I.M. Pidgurskyi, V.V. Slobodyan Finite element analysis of the stress-strain state of perforated steel beams with round unreinforced and reinforced cut-outs. Collection of scientific papers "Resource-efficient materials, structures, buildings and constructions", 2021, vol. 40, pp. 159–165. https://doi.org/10.31713/budres.v0i40.021. (In Ukrainian).

[29] P.O. Martin, M. Couchaux, O. Vassart, A. Bureau An analytical method for the resistance of cellular beams with sinusoidal openings. Engineering Structures, 2017, vol. 143, pp. 113–126. https://doi.org/10.1016/j.engstruct.2017.03.048.

[30] I.M. Pidgurskyi, M.I. Pidgurskyi, O.M. Pidluzhnyi, V.V. Slobodyan Investigation of the shear capacity of beams with single-row and double-row perforations of various configurations / Collection of scientific papers "Urban Development and Spatial Planning", KNUBA, 2021, no. 78, pp. 426–434. https://doi.org/10.32347/2076-815x.2021.78.426-434. (In Ukrainian).

[31] DBN V.2.6–198:2014 Steel structures. Design standards. Kyiv: Minrehion Ukrainy, 2014. 209 p. (In Ukrainian).